Mechanical and Tribological Properties of Graphene Modified Epoxy Composites

Nay Win Khun, He Zhang, Lee Hoon Lim and Jinglei Yang*
School of Mechanical and Aerospace Engineering, Nanyang Technological University, 50 Nanyang Avenue, Singapore 639798, Singapore

* Corresponding author. E-mail: MJLYang@ntu.edu.sg
Received: 17 March 2015; Accepted: 1 April 2015; Published online: 22 April 2015

Abstract
The effects of graphene content on the mechanical and tribological properties of epoxy composites were systematically investigated. The stiffness, hardness and elastic modulus of the composites increased with increased graphene content due to the higher hardness and elastic modulus of graphene sheets than those of epoxy matrix. The friction and wear of the composites measured using steel ball-on-disc microtribological test decreased with increased graphene content due to the solid lubricating effect of graphene sheets. It could be concluded that the mechanical and tribological properties of the epoxy composites could be significantly influenced by the incorporation of graphene sheets.

Keywords: *Epoxy composite, Graphene, Mechanical properties, Friction, Wear*

1 Introduction

Polymers are one of the most successfully exploited materials due to their relatively low cost, facile processing, recyclability and applicability as sustainable materials [1,2]. The specific development of polymer composites based on conventional polymers has drawn much attention to obtain new materials with new structural and functional properties superior to those of pure polymers [1,2]. In addition, polymer composites can achieve the outstanding thermal, optical, electrical, mechanical and tribological properties encountered only with a small quantity of fillers.

Nowadays, polymer composites are widely used for tribological applications because their tribological properties can be tailored using carbon fillers such as carbon nanotubes (CNTs), carbon fibers (CFs), graphene sheets (GSs) and so on [1,3-5]. However, the development of CNT reinforced composites has been impeded by the high cost of CNTs and their difficult dispersion in polymer matrices [1,2]. Recently, graphene has attracted as one of the most popular candidates for the development of structural and functional graphene modified composites because of its high surface-to-volume ratio and outstanding thermal, mechanical, and electrical properties [5,6]. It was reported that improvements in the mechanical and electrical properties of graphene modified polymer composites were much better in comparison to those of clay or other carbon filler based polymer composites [7,8]. Pan et al. [8] studied the tribological performance of graphene modified polyamide coatings and found that the wear resistance of the graphene modified polyamide composite coating was higher than that of neat polyamide coating. It is known that incorporation of graphite particles (GPs) significantly reduces friction of polymer composites via their effective solid lubricating effect [5,6]. However, GSs have less solid lubricating effect than GPs because the GSs possess a smaller number of slip planes. In addition, the tribological behavior of graphene modified epoxy composites during sliding contact with counter metals

Please cite this article as: N. W. Khun, H. Zhang, L. H. Lim, and J. L. Yang, "Mechanical and Tribological Properties of Graphene Modified Epoxy Composites," *KMUTNB Int J Appl Sci Technol*, Vol. 8, No. 2, pp. 101-109, Apr.-June 2015, http://dx.doi.org/10.14416/j.ijast.2015.04.001

is not widely reported. An understanding of a correlation between graphene content in epoxy composites and their tribological properties is important for successful tribological applications.

In this study, epoxy composites with different graphene contents were developed and their mechanical and tribological properties were comprehensively investigated.

2 Experimental Details

2.1 *Sample preparation*

Epoxy resin, Epolam 5015 based on Bisphenol F (Axson Technologies), and related hardener, Hardener 5015 based on the mixture of isophoronediamine and polyoxypropylenediamine (Axson Technologies), were mixed at the recommended ratio of 100:30 to fabricate pure epoxy and epoxy composite samples. For the pure epoxy samples, the epoxy resin and hardener were hand mixed for about 5 min and the mixture was degassed for about 15 min to completely remove air bubbles and then poured into Teflon molds for molding. For the epoxy composite samples, the epoxy resin was first dispersed with GSs (Timesnano, Chengdu) (>98% purity, 2-10 μm diameter, 1-10 layers, 1-3 nm thickness, 330-700 m^2/g specific surface area, 5-10 mg/L tap density) at different concentrations using a mechanical stirrer (Caframo, Model: BDC6015) at 1500 rpm for about 1 h. After evacuation of air bubbles for about 30 min, the dispersion was mixed with the stoichiometric amount of the hardener for about 5 min. The mixture was degassed again for about 15 min before molding. All the molded specimens were cured at room temperature (RT ~ 22-24°C) for 24 h followed by post-curing in an oven (Binder, Model V53) at 80°C for 2 h.

2.2 *Characterization*

The thermal-responsive mechanical properties of the samples with a size of 60 mm × 10 mm × 4 mm, such as stiffness and storage and loss moduli, were diagnosed using dynamic mechanical analysis (DMA) with a bending module at a frequency of 5 Hz from about RT to 195°C.

The hardness and Young's modulus of the samples were measured using a micro-indenter (micro-CSM) with a pyramidal shaped diamond tip of 20 μm in diameter. The indentation test was performed in a load control mode with a total load of 3 N. In each indentation test, the loading and unloading rates and dwelling time at the peak load were 6 N/min, 6 N/min and 5 s, respectively. The hardness and Young's modulus of the samples were derived using Oliver & Pharr's method and averaged from sixteen indentation measurements on each sample [9].

The tensile and compressive properties of the samples were investigated using an universal mechanical tester (Instron 5580) at a cross-head speed of 2 mm/min for both tensile and compressive tests. For the tensile test, three standard dog-bone shaped specimens (prepared according to Type IV in ASTM D638-10) per sample were used to get average tensile breaking stress and Young's modulus. For the compressive test, three cylindrical specimens with a diameter of 12.7 mm and a height of 10 mm per sample were tested to get average compressive breaking stress.

The surface morphology and topography of the samples were studied using scanning electron microscopy (SEM, JEOL-JSM-5600LV) and surface profilometry (Talyscan 150) with a diamond stylus of 4 μm in diameter. For the SEM measurement, the samples were coated with a gold layer to avoid charging. Three measurements on each sample were carried out using surface profilometry to get an average root-mean-squared surface roughness (R_q).

The tribological properties of the samples were tested using a ball-on-disc micro-tribometer (CSM) by sliding them against a 100Cr6 steel ball of 6 mm in diameter in a circular path of 4 mm in diameter for 300 m at different sliding speeds under a normal load of 1 N. All the samples were polished using 1200 grit papers prior to tribological test to stabilize their surface conditions. Three measurements per sample were carried out to get an average friction coefficient. The width and depth of wear tracks were measured using white light confocal imaging profilometry (Nikon L150) to calculate an average specific wear rate.

3 Results and Discussion

Figure 1 shows the DMA results of the epoxy and epoxy composites with different graphene contents. In Figure 1a, the stiffness of the epoxy with 41.52 kN/m

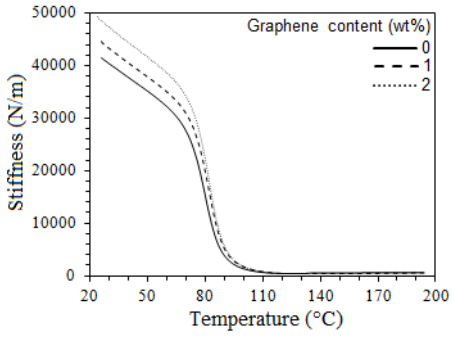

(a)

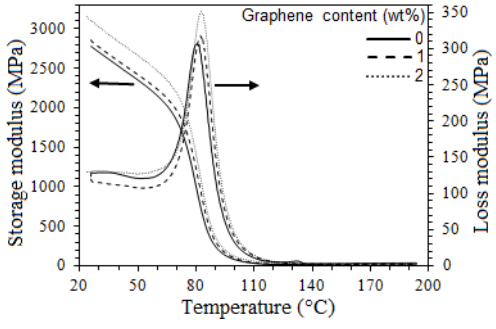

(b)

Figure 1: (a) Stiffnesses and (b) storage and loss moduli of epoxy and epoxy composites with different graphene contents.

at RT significantly decreases with increased working temperature and dramatically drops in the glass transition region and then reaches to about 0.35 kN/m at the temperature of 115°C. The incorporation of GSs in the epoxy apparently improves the stiffness over the wide working temperature range so that increasing the graphene content from 1 to 2 wt% increases the stiffnesses of the epoxy composites at RT and 115°C from about 44.67 and 0.54 kN/m to about 49.34 and 0.67 kN/m, respectively. Such improvement in the stiffness is attributed to the incorporation of rigid GSs in the epoxy matrix [10,11]. In Figure 1b, the increased graphene content increases the storage modulus of the epoxy composites over the wide working temperature range, indicating the improved elastic modulus of the composites. It is found from the curves of loss modulus versus temperature (Figure 1b) that the increased graphene content from 0 to 2 wt% shifts the glass transition temperature (T_g) of the epoxy composites from about 80 to 83°C. It indicates that the glass

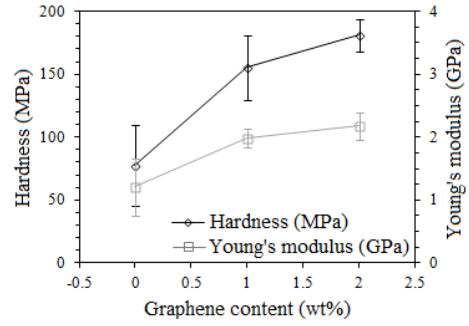

Figure 2: Hardnesses and Young's moduli of epoxy and epoxy composites with different graphene contents.

transtion of the epoxy composites becomes difficult with increased graphene content because the higher graphene content makes the mobility of molecular chains more difficult [12,13].

Figure 2 presents the hardnesses and Young's moduli of the epoxy and epoxy composites with different graphene contents. The increased graphene content from 0 to 2 wt% increases the hardness and Young's modulus of the epoxy composites from about 77.4 MPa and 1.2 GPa to about 181.1 MPa and 2.2 GPa, respectively, probably due to the higher hardness and elastic modulus of GSs than those of the epoxy matrix [10-13].

In Figure 3a, the tensile breaking stresses of the epoxy composites with graphene contents of 1 and 2 wt% are about 68.3 and 67.9 MPa, respectively, while the tensile breaking stress of the epoxy is about 66.7 MPa. Although the tensile breaking stress of the epoxy composites does not significantly change with graphene content, their tensile breaking stresses are slightly higher than that of the epoxy. It indicates that the incorporation of GSs slightly improves the tensile breaking strength of the epoxy composites. In addition, a slightly linear increase in the Young's modulus of the epoxy composites from about 2.65 to 2.83 GPa with increased graphene content from 0 to 2 wt% is found in Figure 3a as a result of the higher elastic modulus of GSs than that of the epoxy matrix. In Figure 3b, the tensile stress of the epoxy linearly increases with increased tensile strain and decreases after the yield point and then sharply drops at the breaking point. However, the increased graphene content apparently decreases the fracture strain of the epoxy composites as shown in Figure 3b, which is indicative of the increased embrittlement of the composites [14].

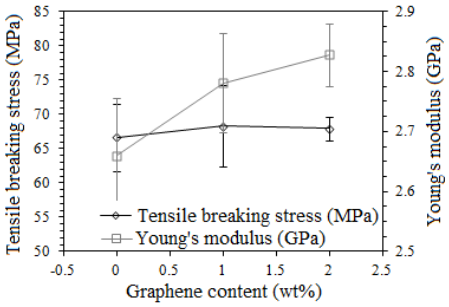

(a)

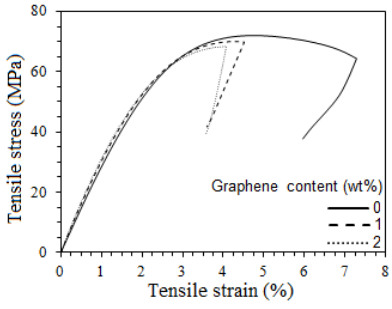

(b)

Figure 3: (a) Tensile breaking stresses and Young's moduli and (b) tensile stress-strain curves of epoxy and epoxy composites with different graphene contents.

Figure 4a shows the fracture morphology of the epoxy, which is perpendicular to the direction of tensile testing, on which fracture lines are apparetnly found. The fracture lines result from fracturing along planes weakened by porosities. However, the fracture morphology of the epoxy composite with the graphene content of 2 wt% is apparently different from that of the epoxy as shown in Figures 4a and b. The incorporation of 2 wt% GSs allows the fracture of the epoxy composite through much smaller planes during the tensile test. Fracturing of embedded GSs is apparently found on the fracture morphology of the epoxy composite with the graphene content of 2 wt% as shown in Figure 4c, which indicates that the relatively good bonding of the GSs with their epoxy matrix is responsible for the slightly higher tensile breaking strengths of the epoxy composites than that of the epoxy.

The compressive breaking stress of the epoxy composites significantly decreases from about 226.1 to 151.2 MPa with increased graphene content from 0 to 2 wt% as found in Figure 5a. It indicates that the

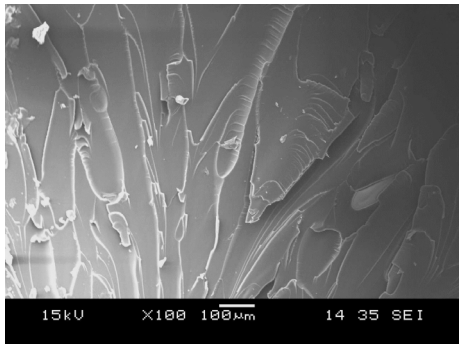

(a)

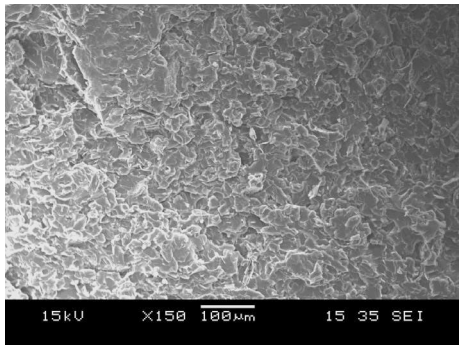

(b)

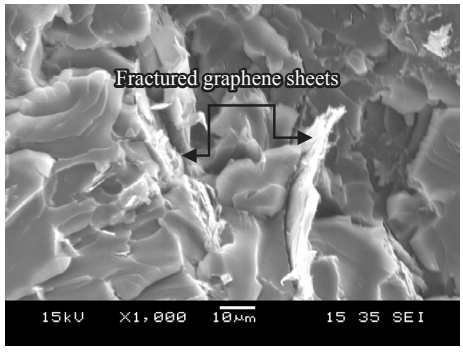

(c)

Figure 4: SEM micrographs showing fracture morphologies of (a) epoxy and (b and c) epoxy composite with graphene content of 2 wt% observed at different magnifications after tensile test.

incresed graphene content decreases the compressive breaking strength of the epoxy composites due to the increased embrittlement of the composites, which is comfirmed by the decreased fracture strain of the composites associated with the increased graphene content as shown in the compressive stress-strain curves of the composites (Figure 5b).

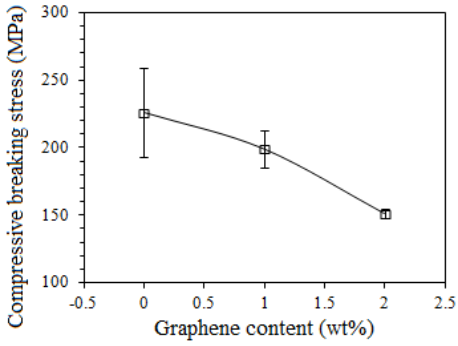

(a)

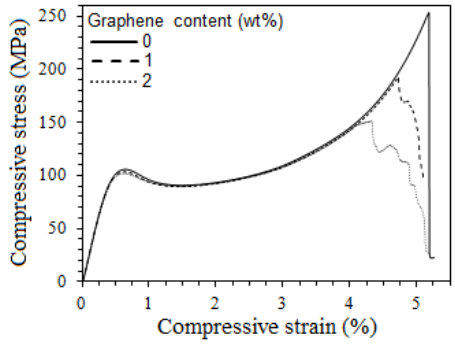

(b)

Figure 5: (a) Compressive breaking stresses and (b) compressive stress-strain curves of epoxy and epoxy composites with different graphene contents.

The surface topographies of the polished epoxy and epoxy composites were measured using surface profilometry. The R_q value of the epoxy is 3.8±0.2 µm as the R_q values of the epoxy composites with the graphene contents of 1 and 2 wt% are 1.8±0.1 and 1.7±0.3 µm, respectively. It indicates that the higher graphene content gives rise to the smoother surface topography of the epoxy composites during the mechanical polishing because the enhanced embrittlement of the composites probably results in an easier fracture of their surface asperities.

Figure 6 consistently shows that the polished epoxy (Figure 6a) has a rougher surface topography than the polished epoxy composite with the graphene content of 2 wt% (Figure 6b). Although abrasive lines caused by the mechanical polishing are apparently found on the surface topographies of the both epoxy and epoxy composite, it can be clearly seen that smaller asperities on the surface of the composite are responsible for its smoother surface topography.

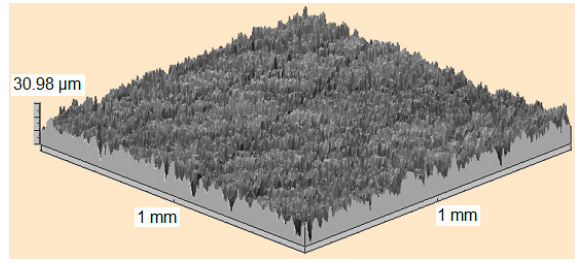

(a)

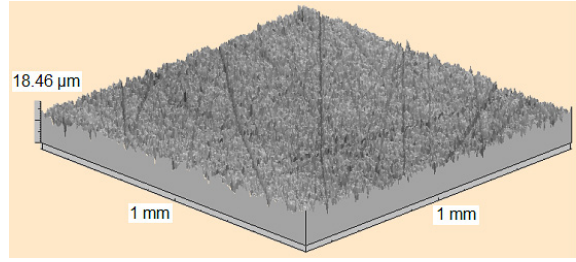

(b)

Figure 6: Surface topographies of (a) epoxy and (b) epoxy composite with graphene content of 2 wt%.

The tribological properties of the epoxy and epoxy composites with different graphene contents were investigated using ball-on-disc micro-tribological test by sliding them against a 6 mm steel ball for 300 m at different sliding speeds under a normal load of 1 N. Figure 7a presents the mean friction coefficients of the epoxy and epoxy composites with different graphene contents tested at different sliding speeds. The friction coefficient of the epoxy tested at the sliding speed of 3 cm/s is about 0.73. However, the incorporation of 1 wt% GSs apparently decreases the friction coefficient of the epoxy composite at 3cm/s to about 0.59 while the increased graphene content to 2 wt% further decreases the friction coefficient to about 0.55. It is clear that the incorporation of GSs apparently decreases the friction of the epoxy composite because the GSs serve as a solid lubricant for the rubbing surfaces [15-19]. In addition, the GSs can serve as spacers to prevent a direct contact between the steel ball and composite [20]. The effect of surface roughness on the friction of the epoxy composites should be taken into account since a rougher surface can generate a higher friction via mechanical interlocking between two mating surface asperities [21-25]. Therefore, the reduced surface roughness of the epoxy composites

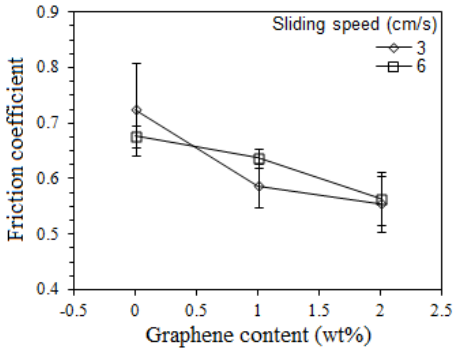

(a)

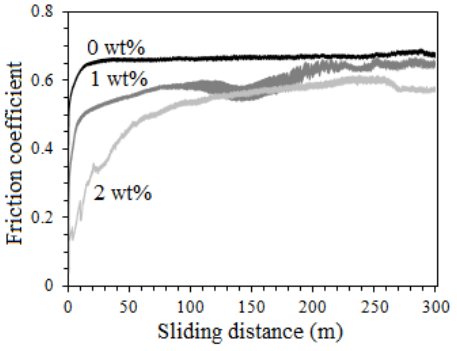

(b)

Figure 7: (a) Friction coefficients of epoxy and epoxy composites with different graphene contents, slid against a 100Cr6 steel ball of 6 mm in diameter in a circular path of 4 mm in diameter for 300 m at different sliding speeds under a normal load of 1 N. (b) Friction coefficients of the same samples, slid at a sliding speed of 3 cm/s, as a function of sliding distance.

with increased graphene content (Figure 6) should be one of the reasons for the decreased friction of the composites (Figure 7a). Since a larger contact between the steel ball and composite can result in a higher friction during sliding contact, the increased stiffness and elastic modulus of the epoxy composites with increased graphene content (Figures 1-3) decrease their friction by reducing their contact with the steel ball [12,22,26-28]. It is consistently found that the friction coefficient of the epoxy composites tested at the sliding speed of 6 cm/s also decreases from about 0.68 to 0.56 with increased graphene content from 0 to 2 wt%.

Figure 7b shows the friction coefficients of the epoxy and epoxy composites tested at a sliding

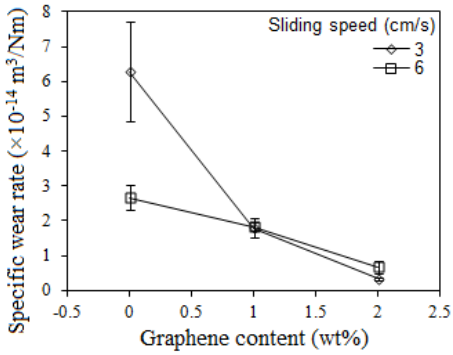

Figure 8: Specific wear rates of epoxy and epoxy composites with different graphene contents.

speed of 3 cm/s as a function of sliding distance. The friction coefficient of the epoxy reaches about 0.65 after sliding for about 20 m and becomes stable at about 0.67 for the rest. Increasing the graphene content apparently decreases the friction coefficient of the epoxy composites during the entire sliding, which confirms that the graphene modified epoxy composites have the lower friction than the pure epoxy.

The mean specific wear rates of the epoxy and epoxy composites with different graphene contents tested at different sliding speeds are presented in Figure 8. At the both sliding speeds of 3 and 6 cm/s, the incorporation of GSs significantly lowers the specific wear rates of the epoxy composites than that of the epoxy as the specific wear rate of the epoxy composites apparently decreases with increased graphene content. The similar trends between the friction (Figure 7a) and wear (Figure 8) of the epoxy composites imply that the frictional behavior of the epoxy composites is closely related to their wear behavior.

Figure 9 shows the wear morphologies of the epoxy and epoxy composite with the graphene content of 2 wt% tested at a sliding speed of 3 cm/s. As shown in Figures 9a and b, the sliding of the steel ball on the epoxy generates an apparent wear track on the surface. The incorporation of 2 wt% GSs apparently lowers the surface wear of the epoxy composite, which is confirmed by a smaller wear track of the epoxy composite (Figure 9c) compared to that of the epoxy (Figure 9a). The repeated sliding of the steel ball produces wear debris via surface wear and compact them to form tribolayers [22,26-28]. Therefore, the formation of tribolayers is clearly found on the wear track of the epoxy composite with

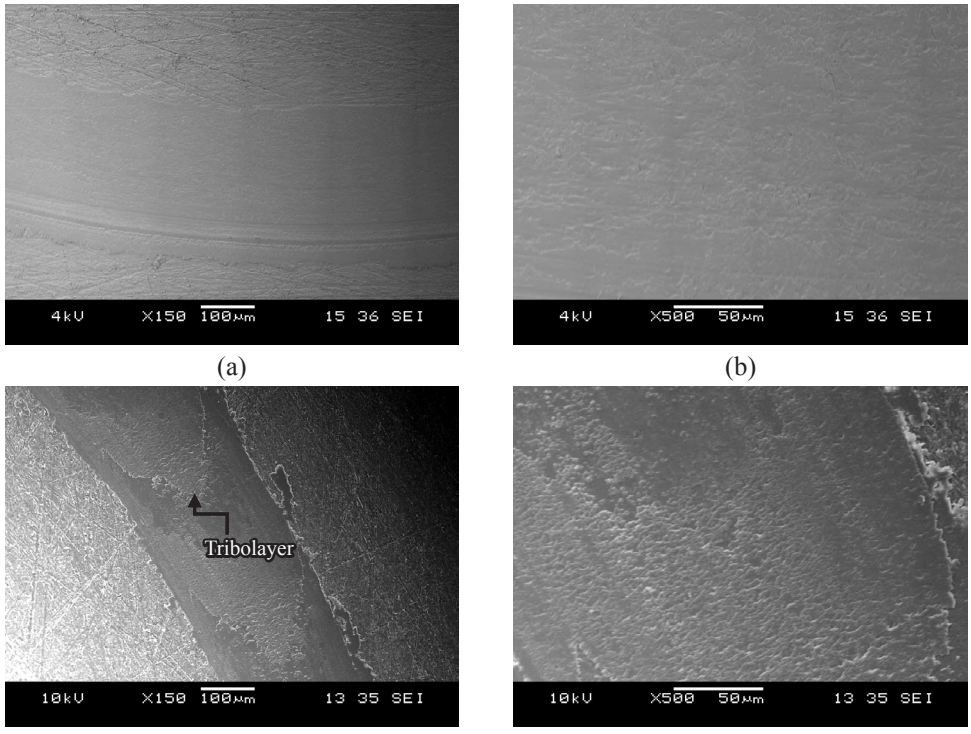

Figure 9: SEM micrographs showing wear morphologies of (a and b) epoxy and (c and d) epoxy composite with graphene content of 2 wt%, slid against a 100Cr6 steel ball of 6 mm in diameter in a circular path of 4 mm in diameter for 300 m at a sliding speed of 3 cm/s under a normal load of 1 N, observed at different magnifications.

the graphene content of 2 wt% (Figure 9c). However, such tribolayers are not apparently found on the wear track of the epoxy because the higher wear of the epoxy does not allow the formation of the tribolayers during the wear test. Micro-wave features can be found on the wear track of the epoxy composite with the graphene content of 2 wt% as shown in Figure 9d. During the repeated sliding, cyclic stress concentration occurred in front of the steel ball initiates minute cracks perpendicular to the sliding direction and propagates them into the subsurface so that the formation of a network of micro-cracks creates the micro-wave features on the wear track (Figure 9d) [29-32]. The formation of the micro-wave features can be correlated to the enhanced embrittlement of the epoxy composite associated with the incorporation of 2 wt% GSs because the micro-wave features are indicative of the surface fatigue. It is further confirmed by the lack of the micro-wave features on the wear track of the epoxy (Figure 9b). It is clear that the formation of tribolayers and micro-wave features give rise to the apparently rougher wear morphology of the epoxy composite (Figures 9c and d) compared to that of the epoxy (Figures 9a and b).

4 Conclusions

The effects of graphene content on the mechanical and tribological properties of epoxy composites were systematically investigated. The DMA results showed that the stiffness and storage modulus of the epoxy composites significantly increased with increased graphene content probably due to the higher elastic modulus of GSs than that of epoxy matrix. It was found from the indentation results that the hardness and Young's modulus of the epoxy composites apparently increased with increased graphene content as a result of the higher hardness and elastic modulus of GSs than those of epoxy matrix. The tensile results indicated that the tensile breaking strengths of the epoxy composites

were slightly higher than that of the epoxy while the increased graphene content increased the Young's modulus of the epoxy composites. The decreased compressive breaking stress of the epoxy composites with increased graphene content was indicative of the increased embrittlement of the composites. The tribological results clearly showed that the increased graphene content decreased the friction and wear of the epoxy composites tested at different sliding speeds due to the solid lubricating effect of GSs. The enhanced embrittlement of the epoxy composites resulted in their surface fatigue wear during the wear test. It could be concluded that the incorporation of GSs could give a significant effect on the mechanical and tribological properties of the epoxy composites.

Acknowledgements

Authors would like to acknowledge the financial support from the Materials Innovation for Marine and Offshore (MIMO) program with the grant number of SERC1123004032 under the Agency for Science, Technology and Research (A*Star) of Singapore.

References

[1] P. M. Ajayan, L. S. Schadler, C. Giannaris, and A. Rubio, "Single walled carbon nanotube polymer composites: Strength and weakness," *Adv. Mater*., vol. 10, pp. 750-753, May 2000.

[2] E. T. Thostenson, Z. Ren, and T. W. Chou, "Advances in the science and technology of carbon nanotubes and their composites: A review," *Compos. Sci. Technol*., vol. 61, pp. 1899-1912, Oct. 2001.

[3] N. W. Khun, B. C. R. Troconis, and G. S. Frankel, "Effects of carbon nanotube content on adhesion strength and wear and corrosion resistance of epoxy composite coatings on AA2024-T3," *Prog. Org. Coat*., vol. 77, pp. 72-80, Jan. 2014.

[4] N. W. Khun, H. Zhang, J. L. Yang, and E. Liu, "Mechanical and tribological properties of epoxy matrix composites modified with microencapsulated mixture of wax lubricant and multiwalled carbon nanotubes," *Friction*, vol. 1, pp. 341-349, Dec. 2013.

[5] N. W. Khun, H. Zhang, L. H. Lim, C. Y. Yue, X. Hu, and J. L. Yang, "Tribological properties of short carbon fiber reinforced epoxy composites," *Friction*, vol. 2, pp. 226-239, Sep. 2014.

[6] H. Quan, B. Q. Zhang, Q. Zhao, R. K. K. Yuen, and R. K. Y. Li, "Facile preparation and thermal degradation studies of graphite nanoplates (GNPs) filled thermoplastic polyurethane (TPU) nanocomposites," *Compos. Part A*, vol. 40, pp. 1506-1513, Sep. 2009.

[7] T. Ramanathan, A. A.Abdala, S. Stankovich, D.A. Dikin, M. H. Alonso, R. D. Piner, D. H. Adamson, H. C. Schniepp, X. Chen, R. S. Ruoff, S. T. Nguyen, I. A. Aksay, R. K. PrudHomme, and L. C. Brinson, "Functionalized graphene sheets for polymer nanocomposites," *Nat. Nanotechnol.*, vol. 3, pp. 327-331, May 2008.

[8] B. Pan, G. Xu, B. Zhang, X. Ma, H. Li, and Y. Zhang, "Preparation and tribological properties of polyamide 11/graphene coatings," *Polym. Plast. Technol. Eng.*, vol. 51, pp. 1163-1166, Jul. 2012.

[9] W. C. Oliver and G. M. Pharr, "An improved technique for determining hardness and elastic modulus using load and displacement sensing indentation experiments," *J. Mater. Res.*, vol. 7, pp. 1564-1583, 1992.

[10] J. C. Wang, P. Chen, L. Chen, K. Wang, H. Deng, F. Chen, Q. Zhang, and Q. Fu, "Preparation and properties of poly(vinylidene fluoride) nanocomposites blended with graphene oxide coated silica hybrids," *Expres. Poly. Lett*., vol. 6, pp. 299-307, Apr. 2012.

[11] T. Kuilla, S. Bhadra, D. Yao, N. H. Kim, S. Bose, and J. H. Lee, "Recent advances in graphene based polymer composites," *Prog. Polym. Sci*., vol. 35, pp. 1350-1375, July 2010.

[12] N. W. Khun and E. Liu, "Tribological behavior of polyurethane immersed in acidic solution," *Tribo. Transac.*, vol. 55, pp. 401-408, Apr. 2012.

[13] K. Gall, M. L. Dunn, Y. P. Liu, D. Finch, M. Lake, and N. A. Munshi, "Shape memory polymer composites," *Acta Mater*., vol. 50, pp. 5115-5126, Dec. 2002.

[14] T. L. Smith, "Volume changes and dewetting in glass bead-polyvinyl chloride elastomeric composites under large deformations," *Trans. Soc. Reology*, vol. 3, pp. 113-136, Jan. 1959.

[15] W. X. Chen, B. Li, G. Han, L. Y. Wang, J. P. Tu, and Z. D. Xu, "Tribological behavior of carbon

nanotube filled PTFE composites," *Tribol. Lett*., vol. 15, pp. 275-278, Oct. 2003.

[16] L. C. Zhang, I. Zarudi, and K. Q. Xiao, "Novel behavior of friction and wear of epoxy composites reinforced by carbon nanotubes," *Wear*, vol. 261, pp. 806-811, Oct. 2006.

[17] C. Li and T. W. Chou, "Elastic moduli of multiwalled carbon nanotubes and the effect of van der Waals forces," *Compos. Sci. Technol*., vol. 63, pp. 1517-1524, Aug. 2003.

[18] W. X. Chen, J. P. Tu, Z. D. Xu, W. L. Chen, X. B. Zhang, and D. H. Cheng, "Tribological properties of Ni-P-multiwalled carbon nanotubes electroless composite coating," *Mater. Lett*., vol. 57, pp. 1256-1260, Jan. 2003.

[19] C. Wang, T. Xue, B. Dong, Z. Wang, and H. L. Li, "Polystyrene-acrylonitrile-CNTs nanocomposites preparations and tribological behavior research," *Wear*, vol. 265, pp. 1923-1926, Nov. 2008.

[20] W. X. Chen, J. P. Tu, X. Y. Gan, Z. D. Xu, Q. G. Wang, J. Y. Lee, Z. L. Liu, and X. B. Zhang, "Electroless preparation and tribological properties of Ni-P-carbon nanotube composite coatings under lubrication condition," *Surf. Coat. Tech*., vol. 160, pp. 68-73, Oct. 2002.

[21] F. Svahn, A. K. Rudolphi, and E. Wallen, "The influence of surface roughness on friction and wear of machine element coatings," *Wear*, vol. 254, pp. 1092-1098, Oct. 2003.

[22] N. W. Khun, H. Zhang, J. L. Yang, and E. Liu, "Tribological performance of silicone composite coatings filled with wax containing microcapsules," *Wear*, vol. 296, pp. 575-582, Aug. 2012.

[23] P. L. Menezes and S. V. K. Kishore, "Influence of surface texture and roughness parameters on friction and transfer layer formation during sliding of aluminum pin on steel plate," *Wear*, vol. 267, pp. 1534-1549, Sep. 2009.

[24] T. S. Barrett, G. W. Stachowiak, and A. W. Batchelor, "Effect of roughness and sliding speed on the wear and friction of ultra-high molecular weight polyethylene," *Wear*, vol. 153, pp. 331-350, Apr. 1992.

[25] M. Clerico and V. Patierno, "Sliding wear of polymeric composites," *Wear*, vol. 53, pp. 279-297, Apr. 1979.

[26] J. M. Thorp, "Abrasive wear of some commercial polymers," *Tribol. Int*., vol. 15, pp. 59-68, Apr. 1982.

[27] N. K. Myshkin, M. I. Petrokovets, and A. V. Kovalev, "Tribology of polymers: adhesion, friction, wear and mass transfer," *Tribol. Int*., vol. 38, pp. 910-921, Nov. 2005.

[28] S. Bahadur, "The development of transfer layers and their role in polymer tribology," *Wear*, vol. 245, pp. 92-99, Oct. 2000.

[29] W. Brostow, H. E. H. Lobland, and M. Narkis, "Sliding wear, viscoelasticity, and brittleness of polymers," *J. Mater. Res*., vol. 21, pp. 2422-2428, Sep. 2006.

[30] X. S. Xing and R. K. Y. Li, "Wear behavior of epoxy matrix composites filled with uniform sized submicron spherical silica particles," *Wear*, vol. 256, pp. 21-26, Jan. 2004.

[31] J. M. Durand, M. Vardavoulias, M. Jeandin, "Role of reinforcing ceramic particles in the wear behavior of polymer based model composites," Wear, vol. 181-183, pp. 833-839, Mar. 1995.

[32] N. W. Khun, H. Zhang, X. Tang, C. Y. Yue, and J. L. Yang, "Short carbon fiber reinforced epoxy tribomaterials self-lubricated by wax containing microcapsules," *J. Appl. Mech*., vol. 81, pp. 121004-1-7, Oct. 2014.